Available online at www.sciencedirect.com
ScienceDirect
European Journal of Pharmaceutics and Biopharmaceutics 64 (2006) 212–221
European Journal of Pharmaceutics and Biopharmaceutics
www.elsevier.com/locate/ejpb

Research paper

Cefdinir: A comparative study of anhydrous vs. monohydrate form Microstructure and tabletting behaviour

Walter Cabri [a], Paolo Ghetti [a], Marco Alpegiani [a], Giovanni Pozzi [a], Angel Justo-Erbez [b], José Ignacio Pérez-Martínez [c,*], Rosario Villalón-Rubio [c], M. Carmen Monedero-Perales [c], Angel Muñoz-Ruiz [c]

[a] *R&D Department, Antibioticos Spa, Rodano (Milan), Italy*
[b] *Institute of Materials Science of Seville, Seville, Spain*
[c] *Department of Pharmacy and Pharmaceutical Technology, University of Seville, Seville, Spain*

Received 28 March 2006; accepted in revised form 15 May 2006
Available online 26 May 2006

Abstract

Anhydrous cefdinir (AC) vs. monohydrated cefdinir (MHC) was compared in order to be used as antimicrobial in therapeutics. Different techniques have been used to characterize physically AC and MHC, and also a complete microstructural analysis of raw materials was carried out. Cefdinir and Maltodextrin QDM® 500 (3:2) formulations were compressed in order to obtain tablets with typical dose of Cefdinir, i.e. 300 mg. Dissolution profiles were obtained for both AC and MHC tablets. Finally tablet X-ray diffraction was performed to ensure the stability of the monohydrated form after tabletting being clearly different in both AC and MHC crystals. AC crystal structure was agreed with the known pattern of anhydrous Cefdinir described in the literature. Microstructural analysis showed large differences in specific surface area (SSA), confirmed by mercury intrusion. Crystal structures of both AC and MHC were stable under mixing, compression and storing processes. Dissolution profiles were faster for hydrate form, probably related to microstructural properties of the crystal which remained after tabletting. In conclusion, it is possible to isolate Cefdinir in two forms anhydrous and monohydrate, well characterized and differentiated. The use of this later improves dissolution of tablet dosage form due to the lack of interconversion during tablet manufacture.

Keywords: Cefdinir; Tablets; X-ray diffraction; Dissolution profiles; Microstructural analysis

1. Introduction

Cefdinir is an orally effective semisynthetic cephalosporin with an extended antibacterial spectrum, and it is characterized by a vinyl group at C-3 and a (*Z*)-2-(2-amino-4-thiazolyl)-2-(hydroxyimino) acetyl moiety at C-7 which result in a marked increase in its antimicrobial activity against Gram-negative and -positive bacteria [1–3] and also enhance its pharmacokinetic properties [4] in the oral route [5]. Fig. 1 shows chemical structure. Anhydrous Cefdinir has been developed and patented by Fujisawa Pharmaceutical in amorphous state [6]. However, the amorphous product has disadvantages in that it is

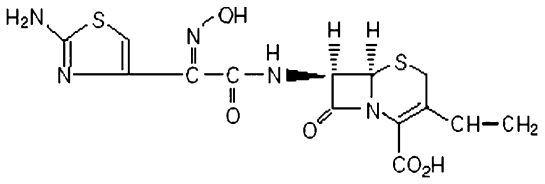

Fig. 1. Cefdinir structure.

* Corresponding author. Department of Pharmacy and Pharmaceutical Technology, Faculty of Pharmacy, University of Seville, C/ Prof. García González, 2, 41012 Seville, Spain. Tel.: +34 954 55 3805; fax: +34 954 55 6726.
E-mail address: jiperez@us.es (J.I. Pérez-Martínez).

0939-6411/$ - see front matter © 2006 Elsevier B.V. All rights reserved.
doi:10.1016/j.ejpb.2006.05.007

bulky, not so pure, unstable and insufficient in filtration rate, therefore is not suitable for a pharmaceutical product [7]. The crystal structure of Cefdinir [7] reported was very pure and stable against heat, light and easy to handle. The crystal structure was described on the basis of X-ray pattern, with distinguishing peaks at the following diffraction angles: [$2\theta(°)$]: 14.7, 17.8, 21.5, 22.0, 23.4, 24.5, 28.1.

Cefdinir may be used in the form of monohydrate as antibiotic [1]. The process for obtaining and isolating Cefdinir in the form of hydrate, e.g. monohydrate, was patented by Sturn et al. [8]. They described a process in which a hydrate is formed by treatment of the Cefdinir dicyclohexylamine salt with an acidic agent. However, the crystalline structure is not given by the corresponding 2θ diffraction angles.

Chemical stability in aqueous media was previously studied [9,10] pointing out degradation via two major degradation routes: lactam ring opening and pH-dependent isomerizations (lactonization, epimerization at C-6 or C-7, *syn–anti* isomerization of *N*-oxime function). However, solid state stability paying special attention to crystalline structure and conditions under which a possible transformation between monohydrate and anhydrous occurs still remains unknown.

The aim of the present paper is to characterize Cefdinir anhydrous (AC) vs. monohydrate form (MHC) by using infrared spectroscopy, Karl Fisher tritimetry, electron scanning microscopy, thermogravimetry, differential scanning calorimetry and X-ray diffraction, as well as to compare microstructure of both raw materials, by nitrogen adsorption and mercury porosimetry. It is also to compare in the present study AC and MHC in tablet dosage form formulations, including tablet compression parameters and dissolution profiles. Finally tablet X-ray diffraction is performed to ensure the stability of MHC after tabletting. This is a novelty in both senses because no previous work has been done with the MHC and all the industrial development of Cefdinir was in the field of hard gelatine capsules, marketed in the US under Omnicef®.

2. Materials and methods

2.1. Materials

Cefdinir, both anhydrous and monohydrate, was supplied from Antibioticos R&D (Milan) Italy:

- Anhydrous Cefdinir: Product R93 Batch 54693
- Monohydrate Cefdinir: Product R93H Batch 52734

Maltodextrin Maltrin QDM® 500 batch 083916V (Grain Processing Corporation, Muscatine, Iowa, USA) is used as direct compression excipient. The choice of this filler was due to the high tablettability [11] and the amorphous nature [12].

2.2. Methods

2.2.1. FT-IR

IR spectra were recorded between 4000 and 450 cm^{-1} by Perkin-Elmer FT-IR spectrometer SPECTRUM 1000 (Norwalk, USA). Each sample was mixed with KBr and compressed at 70kN in a Perkin-Elmer hydraulic press.

2.2.2. Scanning electron microscopy (SEM)

Particle size analysis of samples from batches of powders is examined using a scanning electron microscope Philips XL-30 (Philips, The Netherlands) with the aid of a program of acquisition and reduction of data (Soft-Imaging Software, Münster, Alemania). Several fields were computed for each sample. The following parameters were calculated in the image analysis: average diameter (equivalent circle diameter) and shape factor obtained from the following equation:

$$\text{Shape factor} = 4 * \pi * [\text{area}/(\text{perimeter}\hat{}2)].$$

The particle size distribution of a suitably diluted sample of cefdinir was studied with a Malvern Mastersizer 2000 (Malvern Instruments GmbH, Germany).

2.2.3. Karl-Fisher

An automatic titrator Metrohm 702 SM Titrino (Herisau, Switzerland) with the Hydranal®-Composite (Sigma–Aldrich) and Hydranal®-Methanol Rapid reagents was used for water content determination.

2.2.4. Thermogravimetric analysis (TGA)

A Setaram (Caluire, France) Setsys 1200 system coupled with a personal computer loaded with the program for processing the results was used. Heat and temperature calibration of the instrument was made by high purity indium and zinc as standard samples. The TGA measurements were carried out with platinum sample pan. The heating rate was 10 °C/min from room temperature to 200 °C, under nitrogen atmosphere with a flow rate of 25 ml/min. The mass of the sample was 5–10 mg. All measurements were performed at least in duplicate.

2.2.5. Water uptake

Setaram (Caluire, France) Setsys 1200 was used to obtained water uptake profile under isotherm conditions 25 °C. Atmosphere with a relative humidity 75% was obtained by passing dry nitrogen through water at 20 °C immersed in Julabo (Seelbach, Germany) FP12 bath. TGA oven was cooled by recirculating water bath Julabo (Seelbach, Germany) T1200 which also thermostatised the pipe of inlet gas to avoid nitrogen condensation. The mass of the sample was roughly 50 mg. All measurements were performed at least in duplicate.

2.2.6. Differential scanning calorimetry

A Setaram (Caluire, France) DSC 131 system coupled with a personal computer loaded with the program for

processing the results was used. Heat and temperature calibration of the instrument was made by high purity indium and zinc as standard samples. The DSC measurements were carried out with pierced aluminium sample pans and empty reference pans. Both the sample and reference were scanned at a heating rate of 5 °C/min from room temperature to 300 °C, under nitrogen atmosphere with a flow rate of 25 ml/min. The mass of the sample was 5–10 mg. All measurements were performed at least in duplicate.

2.2.7. Surface area analysis

NOVA 2200 Quantachrome Surface Area Analyzer (Quantachrome, Boynton Beach, FL, USA) was used to measure particle surface area and material density. Weight degassing of samples was carried out by high vacuum (<50μtorr) at 50 °C for 2 h. MultiBET was obtained in the range from 0.05 to 0.3 Nitrogen relative pressure. Nitrogen was of >99.995% w/w purity. The mass of the sample was roughly 1 g. All measurements were performed at least in duplicate.

2.2.8. Material density

Material density reported is obtained by helium filling of the cell and automatic calculation of volume occupied by the powder mass in the cell which volume was previously calibrated. Calculation was done with Software NOVA Enhanced Data reduction Software Ver. 2.13 from Quantachrome.

2.2.9. Mercury porosimetry

Pore size distribution was determined by using a mercury porosimeter (Quantachrome, Boynton Beach, FL, USA) equipped with a Macropore Unit Filling apparatus and a Micropore Autoscan-33. Before analysis, samples were degassed at room temperature for 5 min at high vacuum (<50 μtorr). The maximum intrusion pressure was 33,000 psi. The mass of the sample was roughly 1 g.

2.2.10. Powder X-ray diffraction

X-ray diffraction patterns were obtained with a Siemens Kristalloflex D-5000 diffractometer (Siemens, Haan, Germany). Certain amounts of the samples were analyzed through Bragg geometry in the range from 0° to 70° 2θ. The diffractograms were recorded by using monochromatic CuK_α radiation filtered with Ni. Step was 0.05° and step time was 2 s.

2.2.11. Tabletting

Formulations were prepared by mixing 3:2 Cefdinir and Maltodextrin QDM® 500 in a double-cone Retsch mixer (Haan, Alemania) at 30 rpm during 20 min.

Compression characteristics of the powders were investigated using an instrumented single-punch tablet machine (Bonals model AMT 300, Barcelona, Spain) running at 30 cycles/min, with strain gauges HBM YL6 (HBM, Darmstadt, Germany) and inductive displacement transducers HBM T50; all channels were attached to A/D converter HBM Spider 8. The displacement measurements were corrected with the deformation of punches [13]. An exact amount of 500 mg of powder was manually filled in the die (12 mm). Each tablet contained typical dose of Cefdinir, i.e. 300 mg. Applied pressure was around 150 MPa (tablet hardness – breaking strength – was higher than 100 N). Upper and lower forces as well as punch displacements were monitored during tabletting.

2.2.12. Grazing angle X-ray tablet diffraction

The samples were studied in a Siemens Kristalloflex D-5000 diffractometer (Siemens, Haan, Germany). The radiation used was CuK_α. The grazing angle attachment consisted of a long Soller slit and LiF monochromator, both in the diffracted beam. The measurements were carried out at fixed incident angles ranging from 0.1° to 2°. The instrument was operated in a step-scan mode in increments of 0.05° 2(θ), and counts were accumulated for 2 s at each step.

2.2.13. UV-spectra. Calibration curves

UV spectra were obtained in both water and simulated gastric medium (SGF). Solutions were prepared in the range 0–0.4 mg/mL in order to obtain calibration curve for dissolution testing according to UV–vis Chemstation (Agilent Technologies).

2.2.14. Dissolution profiles

Dissolution profiles were obtained for 6 tablets of each formulation with a USP apparatus 2 consisting of Varian VK 7025 8-spindle dissolution tester (Varian, Weston Park, NC, USA). All studies were run at 50 and 200 rpm. Dissolution was performed using the following medium: water (pH 7.0), SGF pH 1.2 (0.05 N NaCl adjusted to pH 1.2 with HCl). On-line Agilent system monitored continuously drug dissolved by recirculating media from the vessels with a multi-channel peristaltic pump and 8 multi-cell cuvettes (0.1 cm) controlled with the UV–vis Chemstation and the driver for Varian VK7025.

2.2.15. Tablet X-ray diffraction

Tablet X-ray diffraction measurements were made with a Siemens Kristalloflex D-5000 diffractometer (Siemens, Haan, Alemania). A tablet was fixed to sample holder and tablets were analyzed through grazing incidence angle method in the range from 0 to 70 2θ. The diffractograms were recorded by using monochromatic CuK_α and LiF monochromator. Step was 0.05° and step time was 2 s.

3. Results

Fig. 2 shows FT-IR of AC and MHC. Microphotographs of AC and MHC obtained by SEM are shown in Figs. 3A and B, respectively. The average diameters were 21.5 ± 13.1 μm for anhydrous cefdinir and 16.7 ± 10.0 μm for the hydrate, while shape factor was

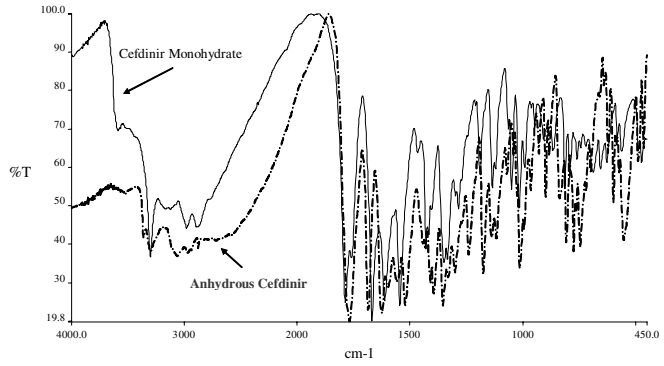

Fig. 2. FT-IR of Cefdinir anhydrous and hydrate.

0.229 ± 0.214 for anhydrous cefdinir and 0.226 ± 0.145 for the hydrate.

Data for particle size distribution obtained from mastersizer support those obtained by SEM. AC shows a bimodal distribution of particle size, with modes at 54.01 and 0.34 μm while MHC exhibits a trimodal distribution of particle size, at 4.38, 43.13 and 0.30 μm.

AC showed water content according to Karl-Fisher of 0.5% w/w while the MHC showed a content of 5.6% w/w.

Fig. 4 shows water uptake profile under isotherm conditions at 75% RH plotted as a function of the temperature.

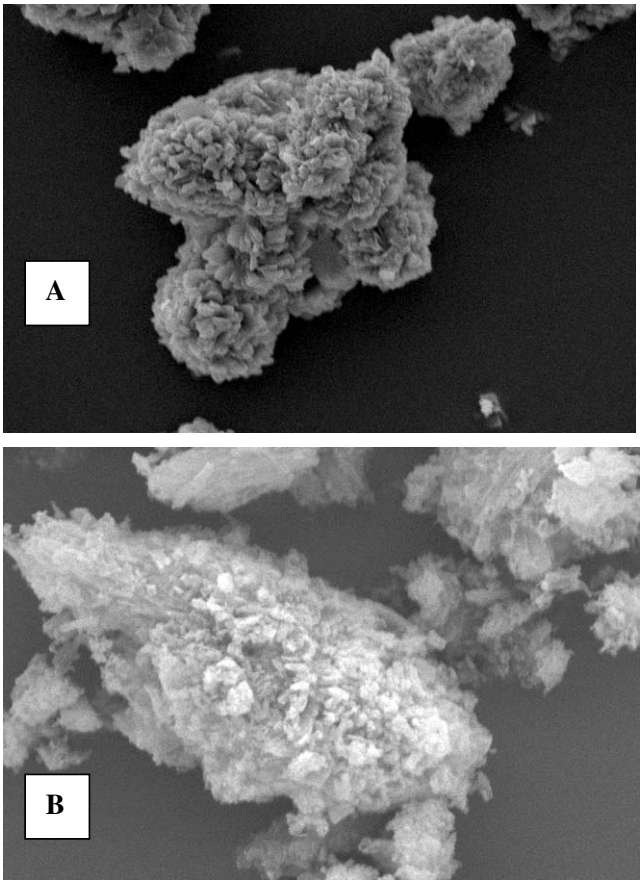

Fig. 3. SEM microphotograph of Cefdinir anhydrous (A) and hydrate (B).

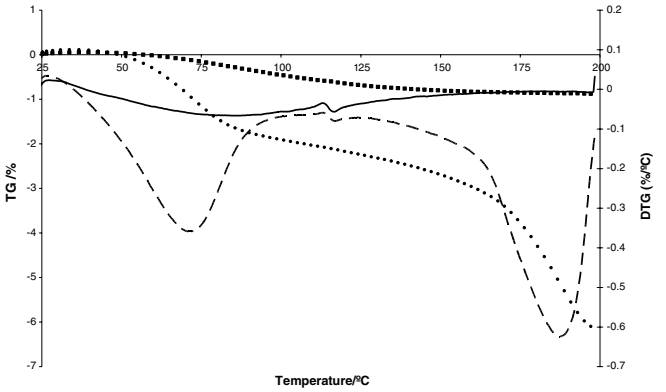

Fig. 4. Thermogravimetric (TG) analysis of Cefdinir anhydrous (circle dots) and hydrate (square dots), derivative thermogravimetric (DTG) analysis of Cefdinir anhydrous (continuous line) and hydrate (discontinuous line).

Curves are shown as thermogravimetric (TG) and differential thermogravimetric profile (DTG) plots for both AC and MHC. The minimum in the curves of DTG profiles were two for the monohydrate (70.89 and 186.30 °C), while in AC was not observed a detectable minimum. Total mass lost between RT and 200 °C was 0.932 for the AC and 6.195% for MHC.

Fig. 5 shows water uptake profile under isotherm conditions at 75% RH as a function of the temperature. Curves are shown as thermogravimetric (TG) and differential thermogravimetric profile (DTG) plots for both anhydrous and hydrate forms. In both cases steady state was reached before 9000 s isotherm experiments. The maximum water uptake was 0.425% for AC and 1.621% for MHC, while maximum DTG was 0.0285%/min for AC and 0.1035%/min for MHC.

Fig. 6 shows DSC curves of both products. Melting curve of AC is described by an onset point of 216.86 °C, peak at 223.82 °C and a total enthalpy of fusion (exothermic) of −439.6 J/g (area under the peak). Pure substances have their melting point at the onset temperature of the melting curve. Thus, the melting point of AC according

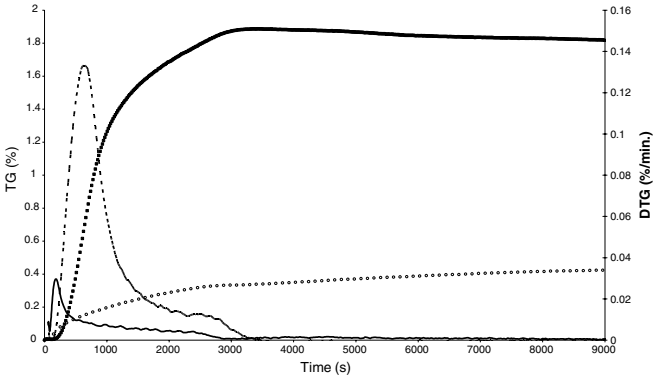

Fig. 5. Water uptake (TG) of Cefdinir anhydrous (square dots) and hydrate (circle dots), derivative water uptake (DTG) of Cefdinir anhydrous (continuous line) and hydrate (discontinuous line).

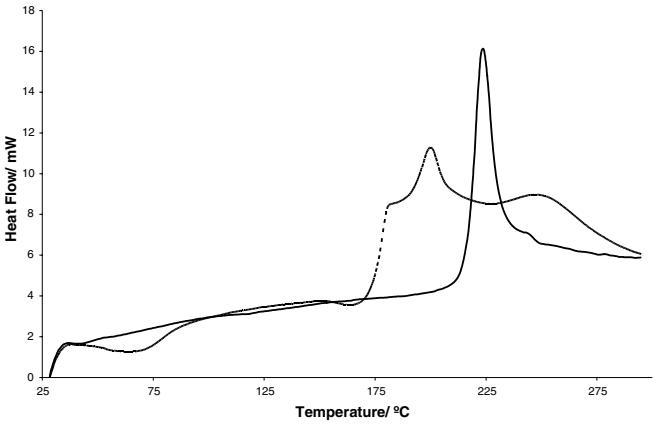

Fig. 6. DSC of Cefdinir anhydrous (continuous line) and hydrate (discontinuous line).

to DSC measurements is 216.86 °C. In the case of MHC form the peak is broadened and with lower vertex temperature with an onset point of 175.32 °C and divided in two peaks at 180.96 and 198.16 °C with corresponding enthalpies of −69.12 and −115.97 J/g.

Table 1 shows specific surface area by MultiBet method calculated with 6 relatives nitrogen pressures in the range between 0.05 and 0.30 in both products in all cases correlation coefficients were higher than 0.999. Single Bet was obtained by highest relative nitrogen pressure of 0.3, while external area was obtained by *t*-method Carbon black [14] for which correlation coefficient obtained was always higher than 0.997. Material density obtained as described in Section 2.2 is shown in Table 1.

Table 2 shows parameters from mercury porosimetric measurements. Bulk or apparent density from mercury intrusion is defined as the volume of the mercury displaced at ambient temperature, while skeletal density is defined as the volume of the mercury displaced at the highest intrusion pressure, i.e. 33,000 psi. This table also shows total intruded volume, pore surface area assuming cylindrical pores open at each radius corresponding to the applied pressure by the Washburn equation and recognizing $2\pi rL$. as pore area [14]. Fractal dimension (D) is calculated from the following equation:

$$\log\left(\frac{dV}{dP}\right) = \log(K_2) + (D-4)\log(P)$$

where K_2 is a proportional constant, V is the intruded volume and P is applied pressure [15]. Thus from the slope of the $\log(dV/dP)$ vs. $\log P$ (range between 1.8 and 4), the fractal dimension could be calculated. In all the cases correlation coefficient was higher than 0.99. Smooth surfaces would present values of $D = 2$, whereas rougher surfaces would present D approaches 3.

Figs. 7A and B show, respectively, the powder X-ray pattern of AC vs. the X-ray pattern [7] previously described.

Mixtures of both anhydrous and hydrate cefdinir forms were prepared and tabletted according to procedures described in Section 2.2. Table 3 shows parameters measured during tablet compression [13] of both mixtures. After tabletting, the grazing incidence X-ray tablet diffraction was used to study crystal structure of Cefdinir and possible transformations during tabletting. Tablets analyzed were intact tablets without either grinding or sectioning may introduce unwanted artefact and further transformations [16]. Fig. 8 shows the X-ray powder diffraction of the Cefdinir anhydrous powder vs. the tablet containing it, while B shows the same comparison for MHC.

Dissolution profiles according to the USP paddle method were obtained for tablet compressed from both Cefdinir anhydrous and hydrate forms. Dissolution testing results in water and SGF (without pepsin) are shown at 50 and 200 rpm in Fig. 9.

4. Discussion

Infrared spectroscopy is a technique being used to measure and identify hydrate and anhydrate forms [17]. Fig. 2 shows FT-IR of both products. Absorbance peaks of water molecules in hydrate form differ from those of the anhydrous form. In the hydrate form characteristic peaks were observed at 1130, 1180, 1665, 1780 and 3300 cm^{-1} this later due to O–H stretching vibration of water molecules [18]. Differences observed between hydrate and anhydrous forms were more pronounced in the range 3800–3100 cm^{-1} according to other studies of drug hydration [19].

SEM showed for both products particles consisting of agglomeration of small plate-like crystals which are scarcely smaller for the hydrate form. The overall shape of the particles was in both cases quite irregular with low values of shape factors.

According to the theoretical value of water content of monohydrate (4.35% w/w) this is lower than the experimental value obtained by Karl-Fisher (5.6% w/w) and with mass loss up to 200 °C (6.2% w/w). These higher

Table 1
Specific surface area and material density of analyzed products

Sample	MultiBET (m^2/g)		SingleBET (m^2/g)		External area (m^2/g)		Density (g/mL)	
	Mean	SD	Mean	SD	Mean	SD	Mean	SD
Cefdinir anhydrous	1.948	0.466	1.867	0.405	2.015	0.558	1.4722	0.0329
Cefdinir hydrate	13.450	0.232	12.800	0.275	13.099	0.438	1.4404	0.0272

Table 2
Parameters from mercury intrusion experiments

Product	Intruded volume (cc/g)		Pore surface area (M2/g)		Fractal dimension		Mean poro size (Å)		Bulk density (g/mL)		Skeletal density (g/mL)	
	Mean	SD	Mean	SD	Mean	SD	Mean	SD	Mean	SD	Mean	SD
Anhydrous Cefdinir	0.678	0.021	3.97	0.17	2.522	0.101	10010	235	0.914	0.025	1.806	0.067
Cefdinir hydrate	0.637	0.035	16.56	0.98	2.845	0.084	1541	54	0.910	0.084	1.800	0.079

experimental values, which are normally observed [18–21], were due to sorbed water, which is more pronounced according to the highly available surface area of the MHC (13.45 m^2/g MultiBet specific surface area). TG curves show water loss from practically room temperature. The water loss comprises two steps according to the two minimum peaks observed from the derivative curve. In the first one water removed is practically sorbed water while in the second one bonded water is being removed. In many cases hydrates show this bonded water in TG curves above 100 °C [18,20,21]. TG profile of AC shows a very low mass in the whole range of temperature most probably related to small amount of sorbed water.

Water uptake of MHC was approximately 10 times higher than that of AC, according to the differences in surface area. The water sorption profiles of the samples under

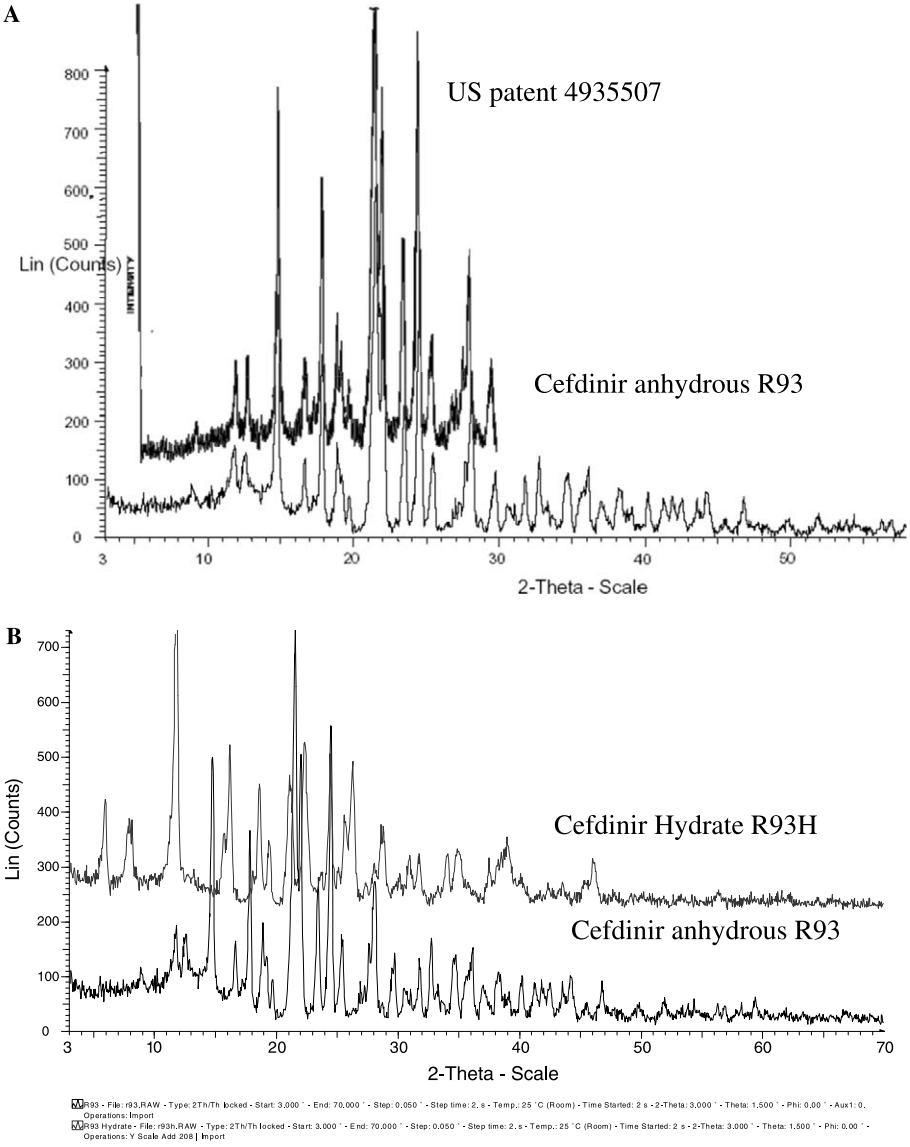

Fig. 7. (A) X-ray powder of Cefdinir anhydrous with the reference X-ray pattern from US Patent 4935507 (1990) and (B) X-ray powder of Cefdinir anhydrous vs. hydrate.

Table 3
Tablet compression parameters

Parameter		Cefdinir anhydrous R93	Cefdinir hydrate R93H
Applied pressure (Mpa)	Mean	127.6	140.5
	SD	0.0	0.3
Applied work (Joules)	Mean	14.15	16.01
	SD	0.86	0.46
Minimum distance between punch tips (mm)	Mean	3.503	3.593
	SD	0.020	0.010
Lubrication coefficient	Mean	0.489	0.510
	SD	0.010	0.020
Maximum ejection force (N)	Mean	4897	2500
	SD	313	283
Plasticity (%)	Mean	99.07	98.62
	SD	0.01	0.01

high relative humidity were obtained after treatment under high vacuum, in which low energy bonded water is removed [22].

DSC of MHC does not show peaks below 175 °C, the low energy necessary for removing sorbed water [21,23] produces only a small increase in baseline over a wide range, this is generally accepted for adsorbed monolayer of water and water tightly bound [21,24]. Furthermore water is strongly bonded and dehydration occurs at temperatures above boiling point of water and close to the melting point of the MHC crystal. DSC in perforated pans produces vapour that cannot escape readily and higher vapour pressure causes water to escape at higher temperatures and different stages [25]. In this case it is difficult to distinguish dehydration and vaporization endotherms [26] MHC shows a double peak in which the release of internal strains left by the crystallization water molecules produces this effect [27].

The specific surface area (SSA) might have direct impact on the dissolution rate, and therefore on the bioavailability of a compound [28]. Analytical principle is the quantification of the N2 volume that can be adsorbed on the surface of the particles from BET equation at different relative pressures – MultiBET – or at the highest relative pressure – SingleBET. Both methods and external Carbon black, and data obtained from mastersizer, show similar tendency, i.e. values six to seven times higher for the monohydrate form. Typical values found for Aventis research compounds were in the range from 0.6 to 5.1 m^2/g [29]. AC was in this range while MHC shows clearly higher SSA. Material density was very similar in both cases. This small difference in material density seems to be more related to hydrate where the water molecules are isolated from the direct contact with other molecules by intervening Cefdinir molecules as occur in cephradine dihydrate [30] similar values were also found for densities derived from mercury intrusion experiments.

Microstructure was also confirmed by mercury intrusion parameters, in this case porosimetry-measured surface area exceeds that of nitrogen adsorption due to ink-bottle-shaped pores having a narrow entrance with a wide inner body [14]. Although the mercury intruded volume per gram was quite similar, large differences were found in mean pore size and fractal dimension. According to mean pore size (on the basis of intruded volume) MHC shows a fine internal structure and taking into account the fractal dimension close to 3 rougher surfaces. Both effects tend to increase dissolution efficiency, especially fractal geometry, as has been stated [31] previously for diclofenac hydroxyethylpyrrolidone.

The powder X-ray diffraction patterns revealed clearly different patterns between AC and MHC, as typically between hydrate and anhydrous forms [32–34]. In the case of AC this matches with the pattern reported in US patent 4935507 [6].

Tablets were compressed at an intermediate applied pressure of 135 MPa (±10%) and breaking strength was in both cases in the range from 60 to 80 N. In order to avoid interference with X-ray patterns maltodextrin was selected as filler and no lubricant was added. This later explains the relatively high friction coefficient and ejection forces [12,13] obtained (Table 3). Grazing angle enabled not only to determine the surface phase composition, but also the profile phase transformation as a function of compact depth [35]. In Cefdinir forms no transformation was observed when powder was compressed into tablets for both AC (Fig. 8A) and MHC (Fig. 8B). Also similar patterns were observed for the two extreme of incidence angles 0.1° and 2°, indicating no modification with penetration depth. According to SEM microphotographs (Fig. 2) particles were irregularly shaped and with a mean particle size smaller than 30 μm. Thus, similar relative intensities could be observed for the raw and the tablet AC (Fig. 8A) and MHC (Fig. 8B) which is related to the random orientation of particles instead of a preferred direction. The differences observed in integrated peak areas and full width at half maximum (FWHM) of raw material and tablets neither demonstrated changes in the microdomains [12]. From these results it appears that AC and MHC remained unaltered after dry blend and tabletting processes.

Dissolution profiles were faster and higher for monohydrate form using water (Fig. 9A) and SGF (9B) media. This is most probably related to the higher surface area of the MHC crystals and which remained after tabletting according to the similar X-ray patterns of the crystals found before and after compression. The intrinsic dissolution profile of cefdinir shows a similar tendency, with a value of 0.05 $mg/min/cm^2$. Compound having polymorphic and/or pseudopolymorphic forms with thermodynamic differences between forms presented differences in solubility and dissolution profiles. In many cases the more hydrated form showed higher stability and slower dissolution curves [18,20,25,27]. However, Cefdinir shows an exothermic heat of fusion which is attached at higher temperature for the AC form. Dissolution profiles of this later did not reach a plateau value from which rate changes progressively to reach the equilibrium rate of the hydrated form [36]. This can be explained by the fact that MHC is not an

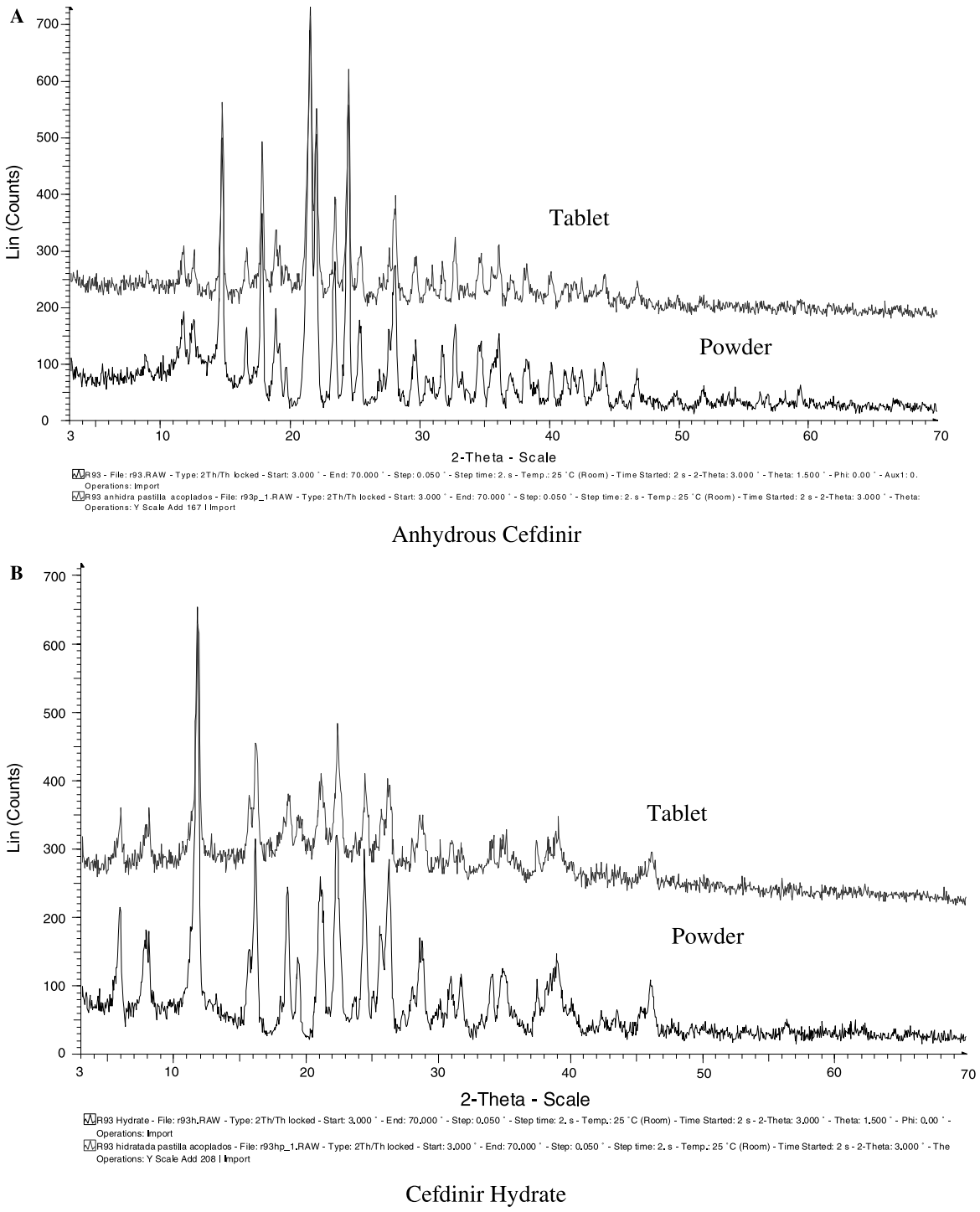

Fig. 8. (A) X-ray powder diffraction of the Cefdinir vs. grazing incidence X-ray diffraction pattern of flat tablet compressed with Cefdinir.

intermediate during dissolution testing of AC. The observed dissolution rate is not affected by the transformation rate due to the low rate of this later process. Dissolution media were chosen without surfactants due to the known effect of wetting, micellar solubilization and deflocculation produced by these which eliminates the ability to distinguish between polymorphic forms [37]. Profiles were faster in acidic medium in which Cefdinir is more soluble than at pH 7.

5. Conclusions

Cefdinir is possible to isolate in two forms anhydrous (AC) and monohydrate (MHC), well characterized by X-ray diffractometry, thermal analysis, tritimetry and infrared spectroscopy. Microstructural properties of the MHC including a very high surface area and a large value of fractal dimension determine dissolution behaviour. The use of MHC to improve dissolution and oral

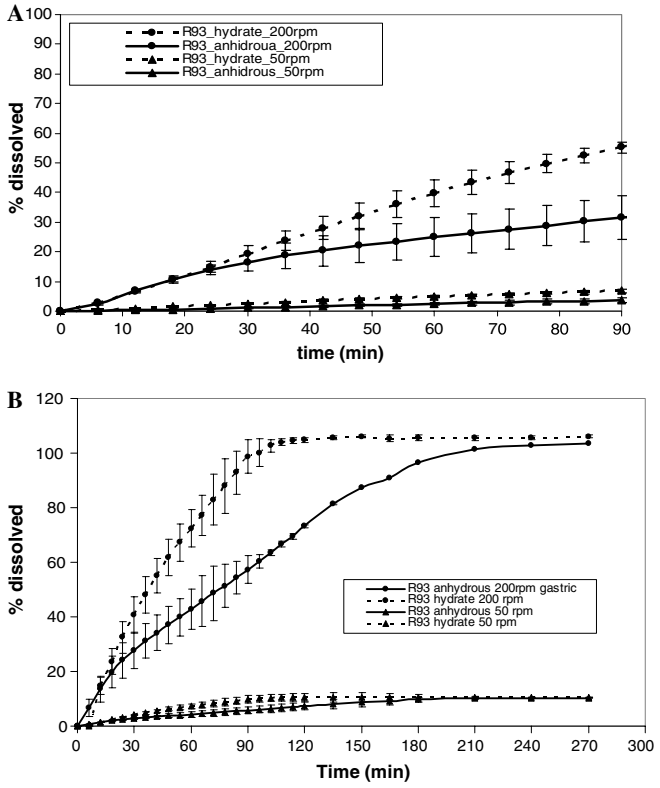

Fig. 9. Comparative dissolution profiles with paddles (USP 2) of both tablet formulations at 50 and 200 rpm in water (A) and simulated gastric fluid (B).

bioavailability overcomes the possibility of interconversion both during manufacture and storage of the tablet dosage form.

Acknowledgements

The authors thank Ministry of Ciencia and Tecnología (Spain) for the support under the auspices of Material Research Program (MAT 2002-02834) and Ministry of Industria for support under PROFIT projects.

References

[1] Y. Inamoto, T. Chiba, T. Kamimura, T. Takaya, FK 482, a new orally active cephalosporin synthesis and biological properties, J. Antibiot. 41 (1988) 828–830.
[2] H.C. Neu, G. Saha, N.X. Chin, Comparative in vitro activity and beta-lactamase stability of FK482, a new oral cephalosporin, Antimicrob. Agents Chemother. 33 (1989) 1795–1800.
[3] Y. Mine, Y. Yokota, Y. Wakai, T. Kamimura, S. Tawara, F. Shibayama, H. Kikuchi, S. Kuwahara, In vivo antibacterial activity of FK482, a new orally active cephalosporin, J. Antibiot. 41 (1988) 1888–1895.
[4] H. Sakamoto, T. Hirose, S. Nakamoto, K. Hatano, F. Shibayama, H. Kikuchi, Y. Mine, S. Kuwahara, Pharmacokinetics of FK482, a new orally active cephalosporin, in animals, J. Antibiot. 41 (1988) 1896–1905.
[5] H. Mikamo, K. Izumi, K. Ito, N. Katoh, K. Watanabe, K. Ueno, T. Tamaya, Study on treatment of bacterial vaginosis with oral administration of metronidazole or cefdinir, Chemotherapy 40 (1994) 362–368.
[6] T. Takaya, H. Takasugui, T. Masugui, H. Yamamaka, K. Kawabata, 7-Substitutes-3-vynil-3-cephem compound and processes for production of the same, US Patent 4,559,334, 1985.
[7] T. Takaya, F. Shirai, H. Nakamura, Y. Inaba, Crystalline 7-(2-(2-aminothiazol-4-YL)-2-Hydroxyiminoacetamido)-3Vinyl-3-cephem-4-carboxylic acid (syn isomer), US Patent 4,935,507, 1990.
[8] H. Sturm, S. Wolf, J. Ludescher, Crystalline amine salt of Cefdinir, US Patent 6,350,869, 2002.
[9] Y. Okamoto, K. Kiriyama, Y. Namiki, M. Fujioka, T. Yasuda, Degradation kinetics and isomerization of cefdinir, a new oral cephalosporin, in aqueous solution 1, J. Pharm. Sci. 85 (1996) 976–983.
[10] Y. Okamoto, K. Kiriyama, Y. Namiki, J. Matsushita, M. Fujioka, T. Yasuda, Degradation kinetics and isomerization of cefdinir, a new oral cephalosporin in aqueous solution. 2. Hydrolytic degradation pathway and mechanism for β-lactam ring opened lactones1, J. Pharm. Sci. 85 (1996) 984–989.
[11] A. Muñoz-Ruiz, M.C. Monedero, M.V. Velasco, M.R. Jiménez-Castellanos, A Physical and rheological properties of raw materials, S.T.P. Pharma Sci. 3 (1993) 307–312.
[12] A. Muñoz Ruiz, T. Payán, A. Justo, M.V. Velasco, M.R. Jiménez-Castellanos, A X-ray tablet and raw diffraction as method to study compression parameters in a direct compression excipients, Int. J. Pharm. 144 (1996) 147–152.
[13] A. Muñoz Ruiz, R. Gallego, R.M. Pozo, M.R. Jiménez-Castellanos, J. Domínguez-Abascal, A comparison of three methods to correct the accuracy of displacement measurements by instrumented single punch tablet machines, Drug Dev. Ind. Pharm. 21 (1995) 215–227.
[14] S. Lowell, J.E. Shield, Powder Surface Area and Porosity, 2nd ed., Chapman and Hall, New York, 1984, pp. 130–141.
[15] D. Avnir, The Fractal Approach to Heterogeneous Chemistry, Wiley, New York, 1989, pp. 78–84.
[16] W. Cao, S. Bates, G.E. Peck, P.L.D. Wildfong, Z. Qiu, K. Morris, Quantitative determination of polymorphic composition in intact compacts by parallel-beam X-ray powder diffractometry, J. Pharm. Biomed. Anal. 30 (2002) 1111–1119.
[17] H.G. Brittain, Spectral methods for the characterization of polymorphs and solvates, J. Pharm. Sci. 86 (1997) 405–412.
[18] S. Ito, M. Nishimura, Y. Kobayashi, S. Itai, K. Yamamoto, Characterization of polymorphs and hydrates of GK-128 a serotonin receptor agonist, Int. J. Pharm. 151 (1997) 133–143.
[19] P. Di Martino, C. Barthélémy, G.F. Palmieri, S. Martelli, Physical characterization of naproxen sodium hydrate and anhydrate forms, Eur. J. Pharm. Sci. 14 (2001) 293–300.
[20] J.M. Rollinger, E.M. Gstrein, A. Burger, Crystal forms of torasemide: new insight, Eur. J. Pharm. Biopharm. 53 (2001) 75–86.
[21] J.L. Ford, P. Timmins, Pharmaceutical Thermal Analysis. Techniques and Applications, Ellis Horwood, Chichester, 1989, pp. 205–220.
[22] K. Umprayn, R.W. Mendes, Hygroscopicity and moisture adsorption kinetics of pharmaceutical solid: a review, Drug Dev. Ind. Pharm. 13 (1987) 653–693.
[23] M.C. Coelho, N. Harnby, Moisture bonding in powders, Powder Technol. 20 (1978) 197–200.
[24] R.J. Khankari, D.J.W. Grant, Pharmaceutical hydrates, Thermochim. Acta 248 (1995) 61–79.
[25] P. Di Martino, F. Piva, P. Conflant, A.M. Guyot-Hermann, Thermal analysis and powder X-ray diffraction study of terpin. Evidence of a eutectic 'hydrate /anhydrous form', J. Therm. Anal. Calorim. 57 (1999) 95–109.
[26] J. Han, R. Suryanarayanan, Applications of pressure differential scanning calorimetry in the study of pharmaceutical Tucker, hydrates I. Carbamazepine dehydrate, Int. J. Pharm. 157 (1997) 209–218.
[27] A. Fini, G. Fazio, A.M. Rabasco, M.J. Fernández, M.A. Holgado, Effect of temperature on a hydrate diclofenac salt, Int. J. Pharm. 181 (1999) 95–106.
[28] R.J. Hintz, K.C. Johnson, The effect of particle size distribution on dissolution rate and oral absorption, Int. J. Pharm. 51 (1989) 9–17.

[29] S. Balbach, C. Korn, Pharmaceutical evaluation of early development candidates "the 100 mg-approach", Int. J. Pharm. 275 (2004) 1–12.
[30] H.G. Brittain, S.R. Byrn, Structural aspects of polymorphism, in: H.G. Brittain (Ed.), Polymorphism in Pharmaceutical Solids, vol. 95, Marcel Dekker, New York, 1999, pp. 73–124.
[31] M.J. Fernández, M.A. Holgado, A.M. Rabasco, G. Fazio, A. Fini, Use of fractal geometry on the characterization of particles morphology. Application to diclofenac hydroxyethylpyrrolidone, Int. J. Pharm. 108 (1994) 187–194.
[32] R.S. Vippagunta, H.G. Brittain, D.J.W. Grant, Crystalline solids, Adv. Drug Delivery Rev. 48 (2001) 3–26.
[33] R. Suryanarayanan, Determination of the relative amounts of anhydrous carbamazepine (C15H12N2o) and carbamazepine dehydrate in a mixture by powder X-ray diffractometry, Pharm. Res. 6 (1989) 1017–1024.
[34] M.S. Kamat, T. Osawa, R.J. DeAngelis, Y. Koyama, P.P. DeLuca, Estimation of the degree of crystallinity of cefazolin sodium by X-ray and infrared methods, Pharm. Res. 5 (1988) 426–429.
[35] S. Debnath, P. Predecki, R. Suryanarayanan, Use of glancing angle X-ray powder diffractometry to depth profile phase transformations during dissolution of indomethacin and theophylline tablets, Pharm. Res. 21 (2004) 149–159.
[36] E. García, S. Vessler, R. Boistelle, C. Hoff, Crystallization and dissolution of pharmaceutical compounds. An experimental approach, J. Crystal Growth 199 (2000) 1360–1364.
[37] E. Swannepoel, W. Liebengerg, M. M de Villiers, Quality evaluation of generic drugs by dissolution test: changing the USP dissolution medium to distinguish between active and non-active mebendazole polymorphs, Eur. J. Pharm. Biopharm. 55 (2003) 345–349.